Plasmonics
DOI 10.1007/s11468-014-9848-3

Dynamically Tunable Plasmonic Lens between the Near and Far Fields Based on Composite Nanorings Illuminated with Radially Polarized Light

Ping Yu · Shuqi Chen · Jianxiong Li · Hua Cheng · Zhancheng Li · Wenwei Liu · Jianguo Tian

Received: 5 July 2014 / Accepted: 25 November 2014
© Springer Science+Business Media New York 2014

Abstract We present a plasmonic lens with a dynamically tunable focal length in the mid-infrared region that is composed of gold film with annular slits and embedded vanadium dioxide (VO_2) nanorings. When illuminated with radially polarized light, a perfect circularly symmetric focusing spot can be dynamically tuned between the near and far fields by decreasing temperature, and it can always be focused beyond the diffraction limit. A physical model of the tunable plasmonic lens is also proposed to explain the mechanisms by which the focal length is dynamically tuned. The field enhancement and the focal length can be further tuned by adding concentric annular slits and VO_2 nanorings, respectively, while keeping the focusing spot size small. This provides a further step in the development of a perfect tunable plasmonic lens.

Keywords Tunable plasmonic lens · Composite nanorings · Radially polarized light

Introduction

The focusing of surface plasmon polaritons (SPPs) has attracted much interest for its great potential in a variety of applications such as high-density optical data storage [1, 2], super-resolution imaging [3, 4], light focusing [5], and plasmonic devices [6, 7]. For these applications, it is important to realize a superior focused spot with perfect size, shape, and strength. Many plasmonic lens designs have emerged to achieve a superior focused spot when excited by linearly polarized light, such as chirped circular nanoslits [8], elliptical nanopinholes [9], and metallic nanoslits with variant widths [10]. However, it is difficult to obtain a single, sufficiently small, and rotationally symmetric spot by using a simple nanostructure with linearly polarized light. This is because not all focused rays have electric field vectors that are essentially parallel to the optical axis in the focal plane. Recently, utilizing the highly symmetrical radially and azimuthally polarized lights to focus the incident light into an ideal spot has become a new central topic of research since vector beams have many more advantages than scalar light for focusing. For instance, vector beams can easily form a focusing spot beyond the diffraction limit due to their special polarization features [11–14]. In addition, radially polarized light can be efficiently coupled with a plasmonic lens to produce brighter and more symmetric focusing spots than those produced by linearly polarized light [15]. Therefore, vector beams have been extensively used to obtain superior focused spots with much smaller size and high intensity. So far, most of the focusing effects observed when using plasmonic lenses have been realized only in the near or far field [16–18], which limits the applications of the plasmonic lens in many domains. The focusing location has to be tuned by accurately modifying the geometry parameters (such as by adjusting the position of the groove outside the slit [19, 20]) or appropriately choosing the materials used to form the plasmonic lens (such as by choosing a different medium in which to immerse the plasmonic lens [21]); this tuning requirement is an inherent drawback. The ability to actively control the resonant constitutive elements of plasmonic lenses will enable the dynamic tunability of their focusing locations between

P. Yu · S. Chen (✉) · J. Li · H. Cheng · Z. Li · W. Liu · J. Tian (✉)
The Key Laboratory of Weak Light Nonlinear Photonics, Ministry of Education, School of Physics and Teda Applied Physics Institute, Nankai University, Tianjin 300071, China
e-mail: schen@nankai.edu.cn
e-mail: jjtian@nankai.edu.cn

Published online: 16 December 2014

the near and far fields. It will also potentially expand the range of applications even further.

Many approaches have been introduced to achieve dynamic tunability of the reaction between structures and incident light with materials such as graphene [22], nonlinear materials [23], and semiconductors [24]. Recently, tunable control of the optical properties of vanadium dioxide (VO_2) has been demonstrated based on its phase transition [25, 26]. The conductivity of VO_2 in the mid-infrared can be easily tuned by changing the room temperature. Therefore, the combination of VO_2 and a plasmonic lens is a promising approach for realizing a dynamically tunable plasmonic lens, which can be widely used in the development of applications such as higher density optical data storage, three-dimensional optical imaging, and three-dimensional optical detectors.

In this letter, we present a plasmonic lens with a dynamically tunable focal length in the mid-infrared region that is composed of gold film with annular slits and embedded VO_2 nanorings. A focusing spot with perfect circular symmetry can be formed when illuminated with radially polarized light. Meanwhile, the sidelobes can be effectively suppressed. The focusing spot can be made dynamically tunable between the near and far fields with decreasing temperature by embedding VO_2 nanorings to form composite nanorings. The spot can always be focused beyond the diffraction limit by tuning the temperature. We also propose a physical model of the tunable plasmonic lens at two particular temperatures to explain the mechanisms by which the focal length is dynamically tuned. The field enhancement can be further improved by adding concentric annular slits, and the focal length can also be extensively tuned by adding VO_2 nanorings while keeping the focusing spot size small.

Focusing Properties of Radially Polarized Light

Figure 1 schematically illustrates the composite nanorings, consisting of a gold film with annular slits and two embedded VO_2 nanorings, which are irradiated by light incident along the z-axis with a wavelength of $\lambda_0 = 3.1$ μm. A 0.6-μm-thick Au-based plasmonic lens with an on-axis hole (0.6 μm in diameter) surrounded by periodic concentric annular slits was deposited onto a glass substrate with a permittivity of 2.25. VO_2 was used to fill in the center hole and the first inner annular slit, which were then simulated with a thermally tunable permittivity ϵ and conductivity σ [27]. The optical constant of gold at 3.1 μm is $\epsilon_{Au} = -433.541 - 24.579i$ [28]. The optimized structure was achieved by using the finite element method (FEM)-based commercial software COMSOL Multiphysics [29]. All boundaries of the computation volume are terminated with perfectly matched layers (PMLs) in order to avoid parasitic unphysical reflections around the composite nanorings. In order to attain a high coupling efficiency, radially polarized incident light is chosen as the optical source due to its ability to illuminate the annular slit with centrosymmetric TM-polarized light. Unlike linearly or circularly polarized beams, the polarization state of radially polarized light is inhomogeneous, so the electric field oscillation trajectory sensitively depends on the locations of the observation points within the beam cross-section. Thus, we consider the vector Helmholtz equation for the electric field [30]

$$\nabla \times \nabla \times \mathbf{E} - k^2 \mathbf{E} = 0, \tag{1}$$

where $k = 2\pi/\lambda$ is the wavenumber. An axially symmetric beamlike vector solution with the electric field aligned in the radial direction should have the form

$$\mathbf{E}(r, z) = U(r, z)\exp[i(kz - \omega t)]\mathbf{e}_r, \tag{2}$$

where $\mathbf{e}_r$ is the unit vector in the radial direction. Substituting Eq. (2) into the vector Helmholtz Eq. (1) and applying the slowly varying envelope approximation (which assumes

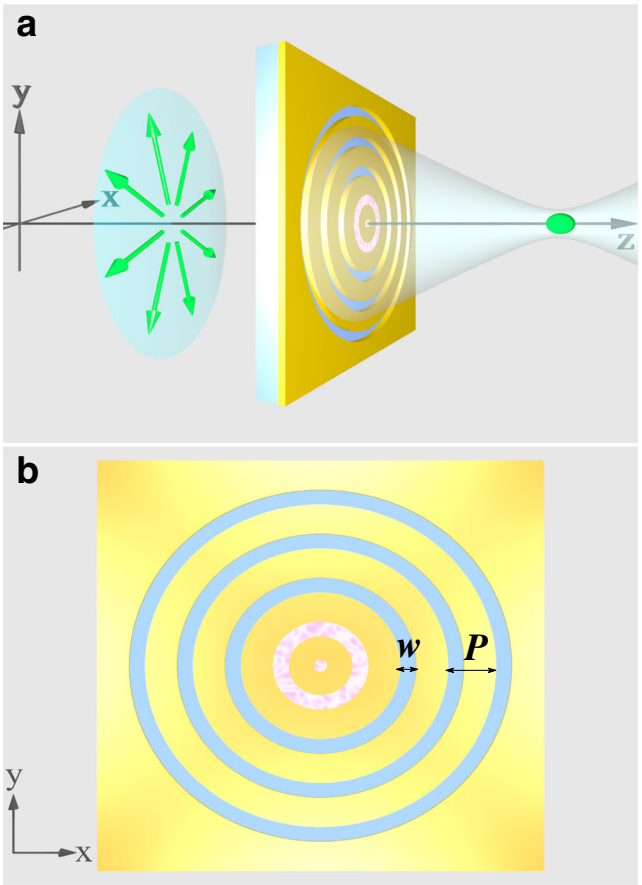

Fig. 1 **a** Schematic model of a plasmonic lens on a substrate under radially polarized incident light and **b** composite nanorings in the x–y plane. The width and period of the annular slits are set to $w = 1$ μm and $P = 3$μm. The numbers of annular slits and VO_2 nanorings are $n_{\text{slit}} = 3$ and $n_{VO_2} = 2$, respectively

that $\frac{\partial^2 u}{\partial z^2} \ll k^2 u$ and $\frac{\partial^2 u}{\partial z^2} \ll k\frac{\partial u}{\partial z}$), $U(r,\ z)$ satisfies the trial solution:

$$U(r,z) = -E_0 J_1\left(\frac{\beta r}{1+iz/z_0}\right)\exp\left[-\frac{i\beta^2 z/(2k)}{1+iz/z_0}\right]u(r,z), \tag{3}$$

where $u(r,\ z) = E_0\frac{w_0}{w(z)}\exp[-i\tan^{-1}(z/z_0)]\exp[i\frac{k}{2(z-iz_0)}r^2]$ is the fundamental Gaussian beam solution, $J_1(x)$ is the first-order Bessel function of the first kind, and E_0 is a constant electric field amplitude. This solution corresponds to a radially polarized vector Bessel-Gauss beam solution. Hence, Eq. (3) represents the radial polarization for the electric field.

Using the radially polarized light to excite the plasmonic lens results in an excellent focusing effect because the surface plasmon can be excited from all directions to form a focusing spot with perfect circular symmetry. We calculated the normalized electric field intensity distributions of nanorings excited by linearly and radially polarized light, and the results are shown in Fig. 2a, b, respectively. The electric field intensity distribution of each focusing spot is asymmetric in the x and y directions when illuminated with x-polarized incident light at a wavelength of 3.1 μm. For radially polarized light at the same wavelength, the normalized intensity of the Bessel-like electric field reaches its maximum at the center of the exit surface, as shown in Fig. 2c. The normalized electric field intensity distributions in the focal plane are also given in the insets of Fig. 2a, b, which further demonstrates the shapes of the focusing spots. To obtain an intuitive comparison of the focusing properties, we present the beam profiles of the focusing region in the x direction for the linearly and radially polarized light, as shown in Fig. 2d. Sidelobes that almost have the same intensity level as the two main focusing spots can be clearly seen when illuminating with linearly polarized light. The normalized electric field intensity excited by the radially polarized light is larger than that excited by the linearly polarized light, and the sidelobes can also be effectively suppressed. These properties of the radially polarized light demonstrate that it has superior capabilities for producing focusing spot.

Dynamically Tuning the Focusing Spot Between the Near and Far Fields

It is known that VO_2 undergoes a metal-semiconductor transition at a critical temperature; this is a first-order structural phase transition from a high-temperature metallic rutile phase to a low-temperature semiconductor monoclinic phase, accompanied by the variation of the material's optical and electric properties. Thus, combining nanorings with VO_2 to form composite nanorings is a promising method for dynamically tuning the focusing properties. Figure 3a–d show the simulated normalized electric field intensity distributions of the presented composite nanorings in the x-z plane illuminated with radially polarized incident light for different temperatures around the transition temperature of VO_2. The variation of the concentration intuitively illustrates that the focusing spot can be dynamically tuned between the near and far fields by decreasing the temperature from 355 K to 343 K. In our work, the far field is

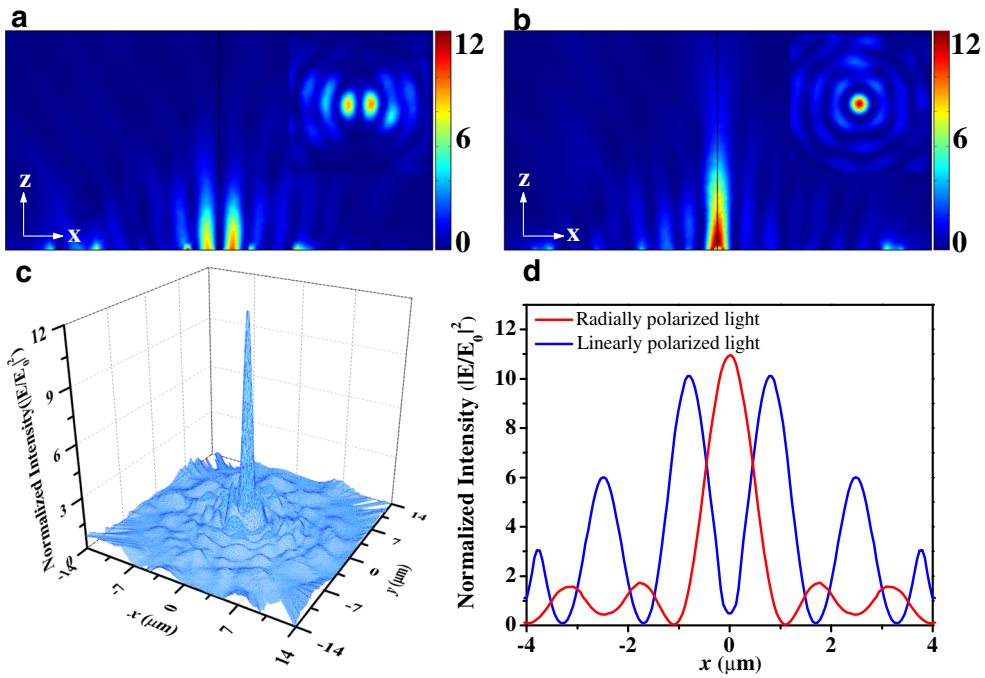

Fig. 2 Normalized electric field intensity distributions of nanorings in the x–z plane illuminated with **a** linearly polarized light and **b** radially polarized light at 3.1 μm. The *insets* show the shapes of the focusing spots in the focal plane. **c** Three-dimensional shape of the focusing spot corresponding to the inset of (**b**). **d** Simulated beam profiles under radially polarized light *(red line)* and linearly polarized light *(blue line)*

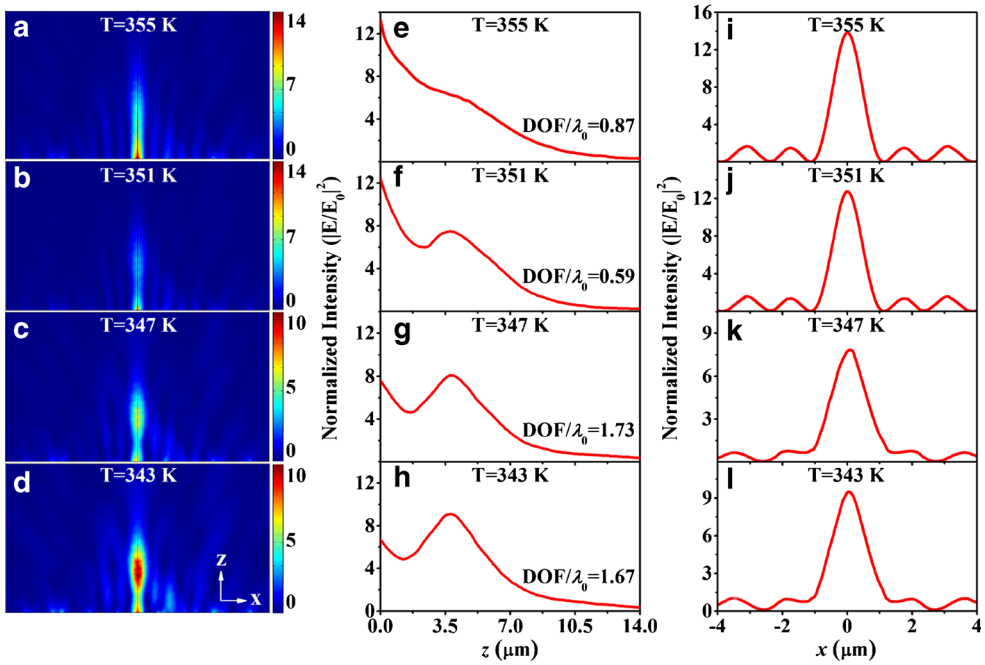

Fig. 3 **a–d** Normalized electric field intensity distributions of composite nanorings in the x–z plane produced by illumination with radially polarized incident light for different temperatures. **e–h** Corresponding intensities along the z-axis. **i–l** Corresponding beam profiles in the focusing region along the x-axis

a relative concept that is defined in comparison with the near field and is used to indicate the focusing region that is farther away from the emitting surface. The incident light at the wavelength of 3.1 μm is closed to the near-infrared wavelength range, and this light has a weak thermal effect. Moreover, the discussed results were obtained under steady-state conditions. The thermal effect caused by light heating will not affect the overall results. Heat balance of the system can be easily achieved by using an external temperature control device in the experiment. In order to more clearly show the transition of the focusing spot, we also calculated the normalized electric field intensity along the optical axis (the z-axis) for different temperatures, and the results are shown in Fig. 3e–h. The results show that the position of the maximal electric field intensity is gradually transferred from the near field to the far field with decreasing temperature. The focusing distances are given in terms of the simulated depth of focus (DOF), which is defined as the full width at half maximum (FWHM) of the central intensity profile along the z-axis. The corresponding values of DOF/λ_0 are shown in Fig. 3e–h. The presented tunable plasmonic lens can realize a large dynamic modulation of the focal length from 0 to 3.9 μm, which may considerably broaden the practical applications of the plasmonic lens in many fields. This tunability is achieved by just changing the environmental conditions, which does not require modifying any parameters or materials of the nanostructure. These advantages make the proposed plasmonic lens more practical and flexible compared with the designs presented in previous works. To show the characteristics of focusing spots in an intuitive way, we present the corresponding beam profiles in the focusing region in Fig. 3i–l. It can be clearly seen that the shapes and sizes of the focusing spots at the corresponding temperatures will not be influenced by adding VO_2 nanorings. In addition, the values of the FWHM of focusing spot along the x-axis, D, produced by illuminating with radially and linearly polarized light, are calculated under a wide range of temperatures from 333 to 361 K, and the results are presented in Table 1. For radially polarized light, the FWHM of the focusing spot, D, can always be focused beyond the diffraction limit by choosing the correct temperature. A minimum spot size D/λ_0 of 0.27 can be achieved at 351 K. For x-polarized incident light, there is no temperature at which the focusing spot can overcome the diffraction limit, where the sizes of the focusing spot in both the x and y directions are larger than those of the spot excited by the radially polarized light.

Table 1 Values of the full width at half maximum (FWHM) of the focusing spots along the x-axis, D, at different temperatures produced by illuminating with radially polarized light (RPL) and linearly polarized light (LPL). The rows labeled LPL_x and LPL_y indicate the values of FWHM of the focusing spots in the x and y directions, respectively, under linearly polarized incident light

D/λ_0	Temperature (K)						
	361	355	351	347	343	339	333
RPL	0.31	0.31	0.27	0.38	0.39	0.39	0.39
LPL_x	0.31	0.31	0.31	0.33	0.35	0.36	0.37
LPL_y	0.52	0.53	0.62	0.64	0.62	0.63	0.64

Physical Mechanisms for Enabling Tunable Plasmonic Lens

As is well known, SPP waves can be scattered into free space by rough surfaces at the metal-vacuum interface [19, 31, 32]. However, perturbation of the surface profile is not the only way to scatter SPP waves. Scattering of SPPs waves can also be caused by surface impedance defects of the metal due to impedance inhomogeneities [33]. To further analyze the physical mechanisms that govern the dynamic tuning of the focal length, we present a physical model of the tunable plasmonic lens at two particular temperatures in Fig. 4. The surface impedance of the proposed composite nanorings varies as the temperature changes. The VO_2 nanorings can be considered to be good conductors when temperature is 355 K. In this case, the plasmonic lens can be considered equivalent to a metal film with three annular slits. Thus, SPP waves with a wavelength of $\lambda_{spp} = \lambda_0\sqrt{\frac{\mathrm{Re}(\epsilon_{Au})+\epsilon_d}{\mathrm{Re}(\epsilon_{Au})\times\epsilon_d}} = 3.09\ \mu m$ can be excited by radially polarized incident light since its wavelength is consistent with the period of the annular slit $P = 3\ \mu m$. Here, ϵ_d is the dielectric constant of air. The SPP waves excited at different slits will have propagation phase differences of $2n\pi (n = 1, 2, 3 \ldots)$. These SPP waves are in phase and constructively interfere with each other to produce a strong field enhancement at the geometrical center, as shown by the arrows in Fig. 4a. Therefore, focusing in the near field can be realized by setting the temperature to a relatively high value. In contrast, the VO_2 nanorings behave as dielectrics when the temperature decreases to 343 K. The plasmonic lens can be considered equivalent to a metal film with two dielectric nanorings and three annular slits. Therefore, the surface impedance is no longer homogeneous in the inner part of the plasmonic lens. This perturbation converts the SPP waves into scattered waves to generate the far field focusing, as shown by the arrows in Fig. 4b. In addition, there is another advantage of using surface impedance instead of surface relief for scattering SPP waves. The dielectric hole/nanorings and annular slits of the composite nanorings will not completely block the light from being transmitted to the other side of the plasmonic lens. The plasmonic lens will transmit both the scattered SPP waves and the strong propagating waves to create the far field focusing.

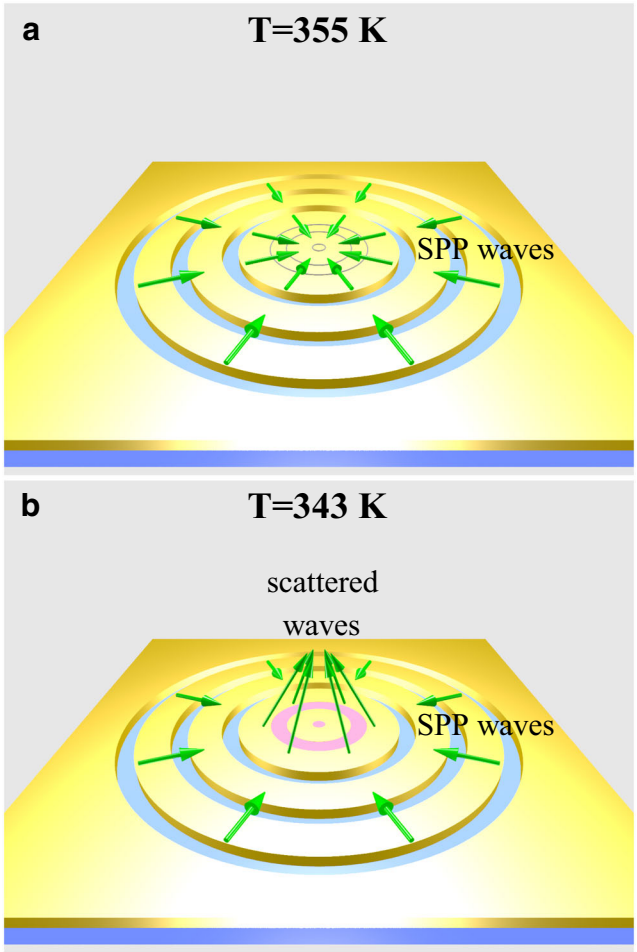

Fig. 4 Physical model of the tunable plasmonic lens for **a** the near field at 355 K and **b** the far field at 343 K. The *green arrows* indicate the directions of the SPP waves and scattered waves

The main function of the annular slits is to convert the incident light into SPP waves that can propagate toward the center of the plasmonic lens. The SPP scattering relies on the existence of the VO_2 nanorings. Therefore, the field enhancement can be further improved by adding additional concentric annular slits with the same period and adding the VO_2 nanorings allows the focal length to be extensively tuned. Figure 5 illustrates the normalized electric field intensities along the optical axis of the composite nanorings with different numbers of annular slits or VO_2 nanorings. Figure 5a, b shows that the focused intensities have been further improved for both the near and far fields by adding another annular slit while keeping the number of VO_2 nanorings constant. Moreover, the focal length can be tuned in a larger range by adding an embedded VO_2 nanoring, as shown in Fig. 5c, d. In order to keep the number of annular slits unchanged, we also added a concentric annular slit at the same time. At a temperature of 355 K, only the SPP waves can be excited, and the maximum intensity still appears in the near field. At a temperature of 343 K, the focal length can be extended to 5.2 μm as the scattering of SPPs is enhanced by adding more VO_2 nanorings. The focused intensities are basically unchanged as the number of annular slits is kept constant, which also confirms the effect of the annular slits. It is worth mentioning that the FWHM values of the focusing spots corresponding to the green lines in Fig. 5a–d are 0.35 λ_0, 0.41 λ_0, 0.36 λ_0, and 0.47 λ_0 respectively, which are still beyond the diffraction limit.

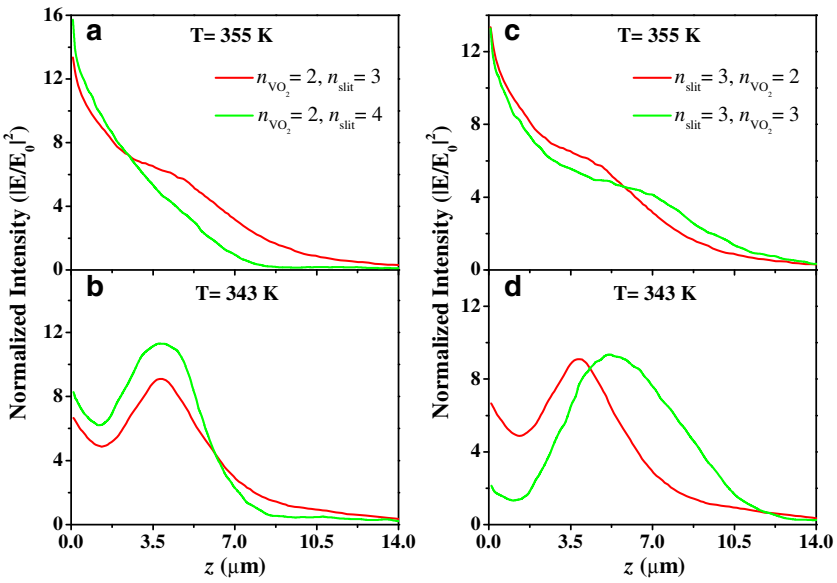

Fig. 5 Normalized electric field intensities of the composite nanorings along the z-axis with different numbers of annular slits(**a** and **b**) and VO_2 nanorings (**c** and **d**) at 355 and 343 K, respectively

Conclusion

In conclusion, we have presented a plasmonic lens that has a dynamically tunable focal length and that is composed of gold film with annular slits and embedded VO_2 nanorings. When the plasmonic lens is illuminated with radially polarized light, the resulting focusing spot, which has perfect circular symmetry, can be dynamically tuned between the near and far fields by decreasing the temperature. To improve the field enhancement (focal length) when using composite nanorings, we have proposed adding more concentric annular slits (more VO_2 nanorings), which can keep the size of the focusing spot small. These properties of the proposed tunable plasmonic lens are of significant importance for applications such as optical data storage, super-resolution imaging, and compact optical devices. As the position of the focusing spot can be flexibly tuned, it is easy to image and detect any region of subjects in both the near field and far field. Therefore, it is expected to be especially useful in a wide range of three-dimensional optical imaging, detection, and electromagnetic sensing.

Acknowledgments This work was supported by the National Basic Research Program (973 Program) of China (2012CB921900), the Chinese National Key Basic Research Special Fund (2011CB922003), the Natural Science Foundation of China (61378006 and 11304163), the Program for New Century Excellent Talents in University (NCET-13-0294), the Natural Science Foundation of Tianjin (13JCQNJC01900), the Specialized Research Fund for the Doctoral Program of Higher Education (20120031120032), and the 111 project (B07013).

References

1. Ditlbacher H, Krenn JR, Lamprecht B, Leitner A, Aussenegg FR (2000) Spectrally coded optical data storage by metal nanoparticles. Opt Lett 25:563–565
2. Zijlstra P, Chon JWM, Gu M (2009) Five-dimensional optical recording mediated by surface plasmons in gold nanorods. Nature 459:410–413
3. Fang N, Lee H, Sun C, Zhang X (2005) Sub-diffraction-limited optical imaging with a silver superlens. Science 308:534–537
4. Smolyaninov II, Hung Y, Davis CC (2007) Magnifying superlens in the visible frequency range. Science 315:1699–1701
5. Lin J, Mueller JPB, Wang Q, Yuan G, Antoniou N, Yuan X, Capasso F (2013) Polarization-controlled tunable directional coupling of surface plasmon polaritons. Science 340:331–334
6. Hutter E, Fendler JH (2004) Exploitation of localized surface plasmon resonance. Adv Mater 16:1685–1706
7. Lerman GM, Yanai A, Ben-Yosef N, Levy U (2010) Demonstration of an elliptical plasmonic lens illuminated with radially-like polarized field. Opt Express 18:10871–10877
8. Fu Y, Liu Y, Zhou X, Xu Z, Fang F (2010) Experimental investigation of superfocusing of plasmonic lens with chirped circular nanoslits. Opt Express 18:3438–3443
9. Fu Y, Zhou X, Zhu S (2010) Ultra-enhanced lasing effect of plasmonic lens structured with elliptical nanopinholes distributed in variant periods. Plasmonics 5:111–116
10. Shi H, Wang C, Du C, Luo X, Dong X, Gao H (2005) Beam manipulating by metallic nano-slits with variant widths. Opt Express 13:6815–6820
11. Zhan Q (2006) Evanescent Bessel beam generation via surface plasmon resonance excitation by a radially polarized beam. Opt Lett 31:1726–1728
12. Luo Z, Kuebler SM (2014) Axial superresolution of focused radially polarized light using diffractive optical elements. Opt Commun 315:176–182
13. Kitamura K, Nishimoto M, Sakai K, Noda S (2012) Needle-like focus generation by radially polarized halo beams emitted by photonic-crystal ring-cavity laser. Appl Phys Lett 101:221103
14. Li Q, Zhao X, Zhang B, Zheng Y, Zhou L, Wang L, Wu Y, Fang Z (2014) Nanofocusing of longitudinally polarized light using absorbance modulation. Appl Phys Lett 104:061103
15. Lerman GM, Yanai A, Levy U (2009) Demonstration of nanofocusing by the use of plasmonic lens illuminated with radially polarized light. Nano Lett 9:2139–2143
16. Chen W, Abeysinghe DC, Nelson RL, Zhan Q (2009) Plasmonic lens made of multiple concentric metallic rings under radially polarized illumination. Nano Lett 9:4320–4325

17. Wang J, Qin F, Zhang DH, Li D, Wang Y, Shen X, Yu T, Teng J (2013) Subwavelength superfocusing with a dipole-wave-reciprocal binary zone plate. Appl Phys Lett 102:061103
18. Chen W, Nelson RL, Zhan Q (2012) Geometrical phase and surface plasmon focusing with azimuthal polarization. Opt Lett 37:581–583
19. Zhang M, Du J, Shi H, Yin S, Xia L, Jia B, Gu M, Du C (2010) Three-dimensional nanoscale far-field focusing of radially polarized light by scattering the SPPs with an annular groove. Opt Express 18:14664–14670
20. Miao J, Wang Y, Guo C, Tian Y, Zhang J, Liu Q, Zhou Z, Misawa H (2012) Far-field focusing of spiral plasmonic lens. Plasmonics 7:377–381
21. Wang EW, Li LL, Yu WX, Wang TS, Gao JS, Fu YQ, Liu YL (2013) The focusing property of immersed plasmonic nanolenses under radially polarized illumination. IEEE Photon J 5:4500207
22. Cheng H, Chen S, Yu P, Li J, Xie B, Li Z, Tian J (2013) Dynamically tunable broadband mid-infrared cross polarization converter based on graphene metamaterial. Appl Phys Lett 103:223102
23. Zharov AA, Shadrivov IV, Kivshar YS (2003) Nonlinear properties of left-handed metamaterials. Phys Rev Lett 91:037401
24. Shen NH, Massaouti M, Gokkavas M, Manceau JM, Ozbay E, Kafesaki M, Koschny T, Tzortzakis S, Soukoulis CM (2011) Optically implemented broadband blueshift switch in the terahertz regime. Phys Rev Lett 106:037403
25. Leahu G, Voti RL, Sibilia C, Bertolotti M (2013) Anomalous optical switching and thermal hysteresis during semiconductor-metal phase transition of VO_2 films on Si substrate. Appl Phys Lett 103:231114
26. Duan X, Chen S, Cheng H, Li Z, Tian J (2013) Dynamically tunable plasmonically induced transparency by planar hybrid metamaterial. Opt Lett 38:483–485
27. Choi HS, Ahn JS, Jung JH, Noh TW (1996) Mid-infrared properties of a VO_2 film near the metal-insulator transition. Phys Rev B 54:4621
28. Lide DR (2001) CRC Handbook of chemistry and physics, 82nd edn. CRC Press, New York
29. COMSOL (2008) Multiphysics 3.4 TM. http://www.comsol.com. Accessed 1 May 2012
30. Zhan Q (2009) Cylindrical vector beams: from mathematical concepts to applications. Adv Opt Photon 1:1–57
31. López-Tejeira F, García-Vidal FJ, Martín-Moreno L (2005) Scattering of surface plasmons by one-dimensional periodic nanoindented surfaces. Phys Rev B 72:161405
32. Yu LB, Lin DZ, Chen YC, Chang YC, Huang KT, Liaw JW, Yeh JT, Liu JM, Yeh CS, Lee CK (2005) Physical origin of directional beaming emitted from a subwavelength slit. Phys Rev B 71:41405
33. Nikitin AY, López-Tejeira F, Martín-Moreno L (2007) Scattering of surface plasmon polaritons by one-dimensional inhomogeneities. Phys Rev B 75:35129